Demixing of severely overlapped H-1 NMR resonances and interpretation of anomalous intensity pattern of dipolar coupled A(3) spins in a weakly aligning medium

ARTICLE *in* JOURNAL OF MAGNETIC RESONANCE · SEPTEMBER 2010

Impact Factor: 2.51 · DOI: 10.1016/j.jmr.2010.08.021 · Source: PubMed

2 AUTHORS:

Nilamoni Nath
Max Planck Institute for Biophysical Chemi…
13 PUBLICATIONS **78** CITATIONS
SEE PROFILE

Suryaprakash Nagarajarao
Indian Institute of Science
106 PUBLICATIONS **709** CITATIONS
SEE PROFILE

Journal of Magnetic Resonance 207 (2010) 190–196

Contents lists available at ScienceDirect

Journal of Magnetic Resonance

journal homepage: www.elsevier.com/locate/jmr

Demixing of severely overlapped ^{1}H NMR resonances and interpretation of anomalous intensity pattern of dipolar coupled A_3 spins in a weakly aligning medium

Nilamoni Nath [a,b], N. Suryaprakash [b,*]

[a] Solid State and Structural Chemistry Unit, Bangalore 560 012, India
[b] NMR Research Centre, Indian Institute of Science, Bangalore 560 012, India

ARTICLE INFO

Article history:
Received 29 May 2010
Revised 30 August 2010
Available online 27 September 2010

Keywords:
Selective excitation
Dipolar couplings
Weakly orienting media
Hetero-decoupling
Chiral discrimination
PBLG

ABSTRACT

We report a single ^{13}C spin edited selective proton–proton correlation experiment to decipher overcrowded ^{13}C coupled proton NMR spectra of weakly dipolar coupled spin systems. The experiment unravels the masked ^{13}C satellites in proton spectrum and permits the measurement of one bond carbon–proton residual dipolar couplings in I_3S and for each diastereotopic proton in I_2S groups. It also provides all the possible homonuclear proton–proton residual couplings which are otherwise difficult to extract from the broad and featureless one dimensional ^{1}H spectrum, in addition to enantiodifferentiation in a chiral molecule. Employment of heteronuclear (^{13}C) decoupling in the evolution period results in complete demixing of overlapped signals from enantiomers. The observed anomalous intensity pattern in strongly dipolar coupled methyl protons in methyl selective correlation experiment has been interpreted using polarization operator formalism.

1. Introduction

Enantiodiscrimination of both naturally occurring and synthetic chiral drug molecules has acquired growing importance because of different biological and chemical properties of enantiomers [1]. Obtaining enantiomerically pure pharmaceuticals is a long standing challenge in asymmetric synthesis. Therefore, identification of enantiomers and their enantiomeric purity measurement from a racemic mixture is of profound importance. In meeting this goal, NMR spectroscopy has proven to be an excellent tool. A wide variety of techniques are available in the literature, which are based on the imposition of diastereomorphic interactions between the enantiomers and chiral derivatizing or solvating agents [2]. Liquid crystalline phase obtained by organic solution of poly-γ-benzyl-L-glutamate (PBLG) with helicogenic solvents, such as, CH_2Cl_2, $CHCl_3$ and DMF has proven to be an efficient medium not only for visualization of enantiomers but also for quantification of excess of one form over the other [3,4]. In such an anisotropic medium, due to differential ordering effect, the order-sensitive NMR observables, viz. chemical shift anisotropy ($\Delta\sigma_i$), dipolar coupling (D_{ij}) and quadrupolar coupling (Q_i) have enormous power of exhibiting different spectrum for each enantiomer enabling their discrimination [4]. Of the several detectable NMR parameters, chiral discrimination in majority of studies is generally monitored either by ^{2}H–{^{1}H} [5] or by two and three dimensional natural abundance deuterium NMR (NAD–NMR) experiments [6–9]. Chiral visualization is also achieved by proton decoupled ^{13}C spectrum deriving advantage of comparatively larger differential values of $\Delta\sigma_{13C}$ between the enantiomers as an alternative tool [10].

The ubiquitous presence of protons in all the chiral molecules, in addition to its high sensitivity renders ^{1}H detection as an advantageous tool. Despite its merits, its detection is methodologically hindered primarily due to the presence of numerous couplings and yields many closely spaced single quantum transitions resulting in the broad and featureless spectrum. In addition, the problem gets severely aggravated due to the superposition of spectra of both the enantiomers. A family of selective excitation experiments employing ^{1}H–^{1}H residual dipolar couplings has partially addressed these difficulties [11–13]. There is also a recent study for selective detection of single-enantiomer spectrum utilizing one dimensional homonuclear correlation of coupled spins [14]. As far as the analyses of the spectrum and the precise determination of only ^{1}H–^{1}H couplings is concerned E-COSY type experiments can also be employed [15,16].

When proton detection provides poor results, either one dimensional ^{13}C coupled proton or proton coupled ^{13}C NMR spectra is an

* Corresponding author. Fax: +91 80 2360 1550.
E-mail address: nsp@sif.iisc.ernet.in (N. Suryaprakash).

1090-7807/$ - see front matter © 2010 Elsevier Inc. All rights reserved.
doi:10.1016/j.jmr.2010.08.021

alternative approach for the measurement of couplings [17,18]. However, the absence of coupling fine structures is most often observed in such spectra and hinders their utilization. This is clearly evident from the proton coupled ^{13}C spectrum of (*R*/*S*)-propylene carbonate aligned in PBLG mesosphere reported in Fig. 1. Quality of the spectrum precludes enantiodifferentiation and the precise measurement of couplings. It is also established that experiments that employ more number of order-sensitive NMR interaction parameters aid in accurate enantiodiscrimination [19]. Therefore, the HSQC type experiments without any decoupling such as F2HSQC and heteronuclear multiple quantum experiments are alternative approaches [19–21]. Both homonuclear and heteronuclear couplings have also been determined using these techniques. The heteronuclear higher quantum experiments suffer from the inherent problem of sensitivity. Also the drawback of F2HSQC experiment is the persistence of spectral complexity in the F_2 dimension.

In the present article, we report ^{13}C satellite spin selective correlation experiment to partially address some of the above-mentioned difficulties. The reported spin state selective correlation is amalgamated with INEPT block to exploit the benefit from both ^{1}H–^{13}C couplings and ^{1}H–^{1}H couplings and also to further enhance the sensitivity [22–26]. The INEPT block helps to retain ^{13}C edited proton magnetization which is subsequently utilized for the selective correlation. This technique, entitled Carbon-13 Edited Spin Selective COrrelation SpectroscopY (CESS-COSY) serves as another alternative approach to obtain both homonuclear and heteronuclear couplings in addition to unambiguous discrimination of enantiomers in a single spectrum. Additionally the incorporation of heteronuclear decoupling in the indirect dimension aids in better enantiodifferentiation. The superiority of this over the methyl selective soft-COSY experiment has also been demonstrated.

2. Experimental confirmation

To explore the applicability of this methodology, three chiral molecules, viz., (*R*/*S*)-2-chloropropanoic acid, (*R*/*S*)-propylene carbonate and (*R*/*S*)-β-butyrolactone, belonging to different NMR spin system nomenclatures have been chosen. The aligned samples were prepared by the well known procedure [4,23]. For the oriented sample (*R*/*S*)-2-chloropropanoic acid, 50 mg of the racemic mixture, 80 mg of PBLG (DP = 782) and 580 mg of $CDCl_3$ were used. For the oriented sample (*R*/*S*)-propylene carbonate, 54 mg of the racemic mixture, 102.8 mg of PBLG, and 665 mg of $CDCl_3$ were used. For the oriented sample (*R*/*S*)-β-butyrolactone, 64.7 mg of racemic mixture, 86.4 mg of PBLG and 432.0 mg of $CDCl_3$ were taken. The assignment of peaks for enantiomers *R* and *S* and to chemically independent proton(s) has already been reported [13–23]. All the spectra were recorded using a Bruker DRX-500 NMR spectrometer. The designed pulse sequences are reported in Fig. 2. For selective excitation, SEDUCE, EBURP-2 and U-BURP shaped pulses were utilized. The experimental and processing parameters including the appropriate delays responsible for polarization transfer are reported in Table 1. The determined coupling parameters are contained in the respective figure captions.

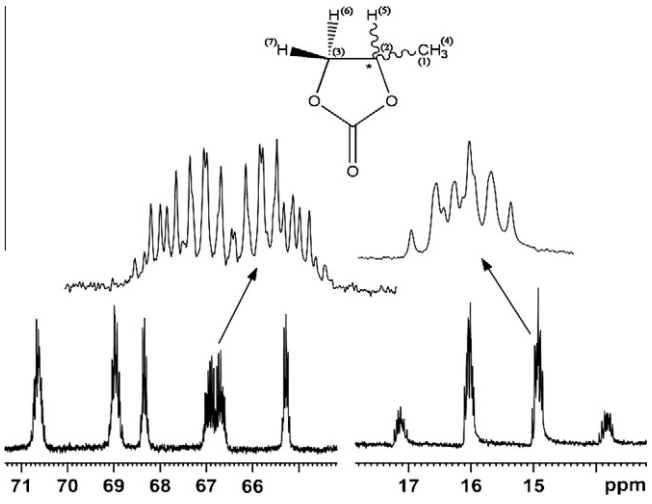

Fig. 1. ^{1}H coupled one dimensional ^{13}C spectrum of (*R*/*S*)-propylene carbonate aligned in the PBLG liquid crystalline solvent, recorded at 300 K. The chemical structure and the numbering of the interacting spins of the molecule are given at the top of the spectrum. The crowded regions are expanded to depict the spectral complexity and indistinguishable overlap of spectra of enantiomers.

3. Polarization operator description of an expected multiplet pattern

To analyze the multiplet pattern originating from a weakly dipolar coupled seven spin system of the type A_3MNPX, [where *X* being the natural abundance ^{13}C attached to methyl (A_3) protons, the remaining spins are protons, with *N* and *P* being diastereomeric protons] with the present pulse scheme (Fig. 2A), the polarization operator formalism [27] has been employed. The present seven

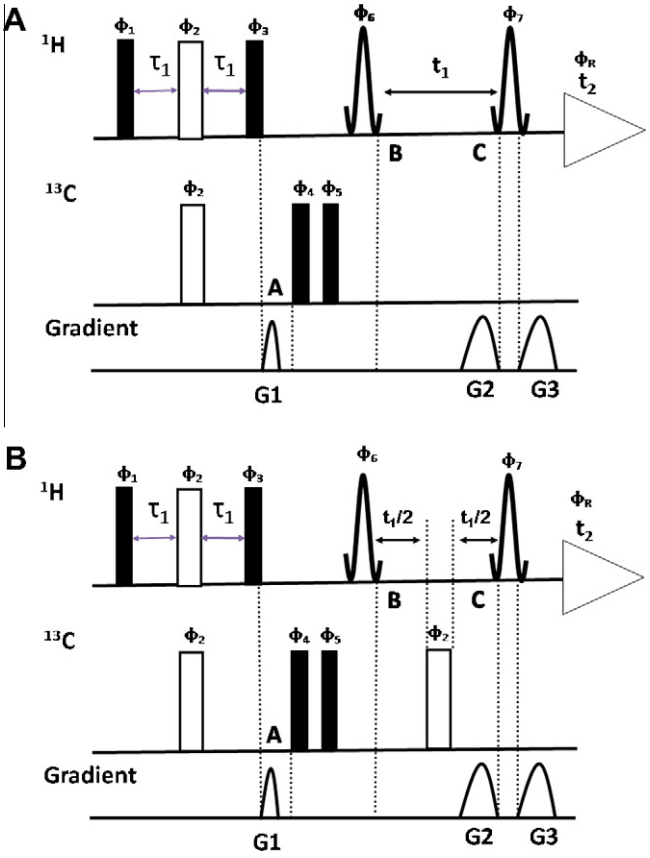

Fig. 2. (A) The pulse sequence employed for CESS-COSY. The spin dynamics during different time periods of the pulse sequence are discussed in the text. Filled rectangular bars are hard 90pulses and empty rectangular bars are hard 180 pulses. All the remaining pulses are semi-selective for the excitation of multiplets. (B) The pulse sequence used for the ^{13}C–^{1}H decoupling in the indirect dimension in CESS-COSY. In both the sequences the pulse field gradient (G1) applied after keeping the longitudinal term acts as a z purge to dephase undesired coherences. The delay τ1 responsible for the polarization transfer depends on the factor $1/(4(^{1}T_{AX}))$ and was optimized for each molecule independently, the gradient ratio employed was G2:G3 = 1:1. The phases of the pulses are; $\varphi_1 = x$, $\varphi_2 = 4(x),4(-x)$; $\varphi_3 = y$; $\varphi_4 = \varphi_7 = 4(x)\ 4(-x)$; $\varphi_5 = 2(x, -x)$; $\varphi_6 = 2(x), 2(-x)$ and $\varphi_R = x, 2(-x), x-x, 2(x), -x$.

Table 1
Acquisition and processing parameters employed for the two-dimensional CESS-COSY experiments in (*R*/*S*)-2-chloropropanoic acid, (*R*/*S*)-propylene carbonate and (*R*/*S*)-β-butyrolactone aligned in PBLG/$CDCl_3$ mesophase.

Parameters	(*R*/*S*)-2-chloropropanoic acid		(*R*/*S*)-propylene carbonate		(*R*/*S*)-*β*-butyrolactone	
	F_1 dimension	F_2 dimension	F_1 dimension	F_2 dimension	F_1 dimension	F_2 dimension
Spectral width (Hz)	320	320	290	290	600	600
Number of data points	1k	196	1k	200	2k	400
Digital resolution (Hz)	0.15	0.62	0.13	0.56	0.14	0.58
Zero filling of data	8k	4k	4k	2k	8k	4k
Window function	SINE	SINE	SINE	SINE	SINE	SINE
SEDUCE shaped pulse length (ms)	1.66		3.12		3.5[a]	
Optimized 'τ' delay (ms)	1.92		1.18		1.2	
Relaxation delay (s)	2		2.5		2.7	
Number of accumulations	8		8		8	

[a] Selective pulse of identical duration is applied at two groups of frequencies pertaining to protons H5 and H6 to achieve biselective excitation.

spin system contains IS, I_3S and I_2S groups. Spectrum of such a spin system is influenced by homonuclear couplings, viz. $^2T_{AA}$, $^3T_{AM}$, $^4T_{AN}$ and $^4T_{AP}$ and one heteronuclear coupling $^1T_{AX}$ (where $T_{ij} = J_{ij} + 2D_{ij}$ for nonequivalent spins and $T_{ij} = 3D_{ij}$ for equivalent spins and the superscript pertains to the coupled proton that is separated by that many bonds). Since the first selective pulse has been applied only on A_3 spins and ^{13}C being the rare spin, the heteronuclear couplings, $^2T_{MX}$, $^4T_{NX}$ and $^4T_{PX}$ are undetectable.

For the chosen spin system, the product operator $2A_{(1)z}X_z$ is present after the application of second non-selective 90° pulse on protons. The coherence transfer pathway from the time point A–B can be written as

$$2A_{(1)z}X_z \overset{(\pi/2)_x^X}{\rightarrow} -2A_{(1)z}X_y \overset{(\pi/2)_x^X}{\rightarrow} -2A_{(1)z}X_z \overset{(\pi/2)_x^X}{\rightarrow} 2A_{(1)y}X_z \quad (1)$$

In the t_1 dimension, $A_{(1)}$ experiences the coupling to $A_{(2)}$, $A_{(3)}$, *M*, *N*, *P* and *X* spins. The nomenclature $A_{(1)}$, $A_{(2)}$ and $A_{(3)}$ correspond to three individual methyl protons. The spin system in this dimension pertains to A_3MNPX where A_3's are active spins, *M*, *N*, *P* and *X* constitutes passive spins. Therefore, the term $2A_{(1)y}X_z$ which is present in the indirect dimension could be expressed in terms of polarization operator product (i.e. $A_{(1)y}E_{(2)}E_{(3)}E_ME_NE_PX_z$) as;

$$\frac{1}{32i}[A_{(1)-}(A_{(2)\alpha}+A_{(2)\beta})(A_{(3)\alpha}+A_{(3)\beta})](M_\alpha+M_\beta)(N_\alpha+N_\beta)(P_\alpha + P_\beta)(X_\alpha - X_\beta) \quad (2)$$

The terms inside the square bracket, that are coupled to the passive spins are

$$A_{(1)-}A_{(2)\alpha}A_{(3)\alpha}, \quad A_{(1)-}A_{(2)\alpha}A_{(3)\beta}, \quad A_{(1)-}A_{(2)\beta}A_{(3)\alpha} \quad \text{and} \quad A_{(1)-}A_{(2)\beta}A_{(3)\beta}$$

Of these four terms, the second and third terms being degenerate, possess identical frequencies and hence these four terms give rise to a triplet. Since in PBLG/$CDCl_3$ solvent generally $^1T_{AX} > {}^2T_{AA}$, first the $A_{(1)-}$ single quantum term is initially split into a doublet with larger separation due to spin states $|X_\alpha\rangle$ and $|X_\beta\rangle$. Each component of the doublet is further split into a triplet because of the coupling of A_3 to *X* spin. Consequent to the coupling of A_3 to *M*, *N* and *P* spins, each component of triplet of a doublet is further split into a doublet of doublet of a doublet in each spin state of *X*, i.e. $|X_\alpha\rangle$ or $|X_\beta\rangle$ states due to eight possible spin states of *M*, *N* and *P*., viz. $|M_\alpha N_\alpha P_\alpha\rangle$, $|M_\beta N_\alpha P_\alpha\rangle$, $|M_\alpha N_\beta P_\alpha\rangle$, $|M_\alpha N_\alpha P_\beta\rangle$, $|M_\beta N_\beta P_\alpha\rangle$, $|M_\beta N_\alpha P_\beta\rangle$, $|M_\alpha N_\beta P_\beta\rangle$ and $|M_\beta N_\beta P_\beta\rangle$. Thus, triplets appear in eight cross sections in either $|X_\alpha\rangle$ or $|X_\beta\rangle$ states. The spectrum appears as an arrays of triplets with the displacement between cross sections providing information on passive couplings. The spectrum remains identical in both the dimensions. On the other hand, the heteronuclear coupling ($^1T_{AX}$) is absent in the indirect dimension of the pulse sequence depicted in Fig. 2B, which is accomplished by the application of the π pulse at the centre of evolution period on the ^{13}C spin. Therefore, the spectrum in the indirect dimension is different from that in the direct dimension which is a doublet of a doublet of doublet of a triplet.

4. Results and discussion

4.1. Application to (R/S)-2-chloropropanoic acid

For the demonstration of experimental methodologies, the chiral molecule (*R*/*S*)-2-chloropropanoic acid aligned in PBLG/$CDCl_3$ was investigated. This molecule has been chosen as the spin system is simple and it provides better insight into the pulse sequence. The chemical structure, the numbering of interacting spins of the molecule and the methyl selective 2D CESS-COSY spectrum obtained at 300 K are reported in Fig. 3A. The high resolution achieved and the efficient suppression of the proton peaks attached to ^{12}C is clearly evident. In this experiment the spin systems in both the dimensions pertain to A_3MX where A_3 are the active spins, *M* and *X* are passive spins. Methyl protons gives rise to a triplet with active coupling $^2T_{H4H4}$ which is further split by $^1T_{C1H4}$, another active coupling of large strength. The spectrum can be construed as an arrays of four A_3 sub-spectra in both the dimensions pertaining to four passive spin states of M and X for each enantiomer. The displacement between two identical cross sections belonging to the $|\alpha\rangle$ and $|\beta\rangle$ domains of ^{13}C provides $^1T_{C1H4}$. The separations marked "*a*" and "*b*" pertain respectively to the active couplings $(^1T_{C1H4})^{R/S}$. It is appropriate to mention that analysis of the spectrum at any one of the spin states of ^{13}C is sufficient to derive all homonuclear couplings. The expanded region corresponding to $|\alpha\rangle$ spin state of ^{13}C, reported in Fig. 3B, contains markings of separations that provide homonuclear couplings. Separations between adjacent transitions of the triplets marked as *c* and *e* provide respectively the active couplings $(^2T_{H4H4})^{R/S}$. The passive couplings $(^3T_{H4H5})^{R/S}$ are obtainable from the displacements *d* and *f*, respectively.

4.2. Anomalous intensity pattern of strongly coupled A_3 group

The inspection of the methyl selective spectrum in Fig. 3B reveals the steady decrease in the intensity of transitions from the shielded to deshielded region or vice versa depending on the spin states of the passive spins. The cross sections marked (i) and (ii) for *R* enantiomer (Fig. 4A) show reverse trend of change in intensities for the passive spin states $|M_\alpha X_\alpha\rangle$and$|M_\beta X_\alpha\rangle$. Similar trend is also observed for cross section marked as (iii) and (iv) for *S* enantiomer. This typical spectral pattern is observed in all the investigated molecules possessing the methyl group. The anomolous intensity pattern could be understood by considering an SQ coherence term, such as, $A_{(1)+}A_{(2)\alpha}A_{(3)\alpha}M_\alpha X_\alpha$. For brevity the $A_{(1)+}A_{(2)\alpha}A_{(3)\alpha}$ component of this SQ is considered in the following discussion.

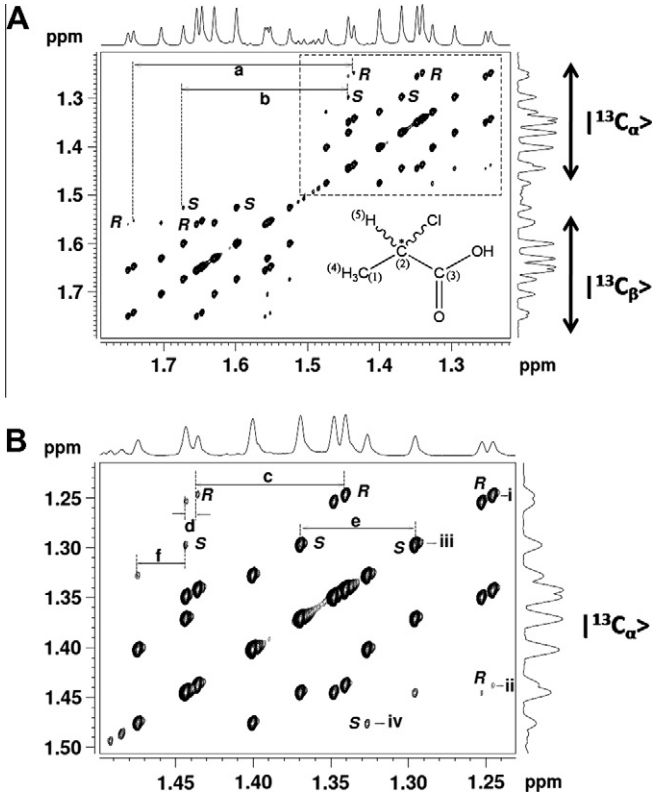

Fig. 3. (A) The selective methyl protons excited 2D CESS-COSY spectrum of (*R*/*S*)-2-chloropropanoic acid aligned in the liquid crystalline solvent PBLG/ $CDCl_3$, recorded at 300 K. $|^{13}C_\alpha>$ and $|^{13}C_\beta>$ regions are marked in the F_1 dimension. The structure and the numbering of coupled spins of the molecule are given as an inset. Few representative peaks for *R* and *S* enantiomers are marked. (B) The expanded $|^{13}C_\alpha>$ region of Fig. 3A. The magnitudes of the couplings (in Hz) are; $a = (^1T_{CH})^R = 153.3$, $c = (^2T_{HH})^R = 45.3$, $d = (^3T_{HH})^R = 3.9$ and $b = (^1T_{CH})^S = 114.6$, $e = (^2T_{HH})^S = 38.0$ and $f = (^3T_{HH})^S = 15.7$.

The mixing pulse creates SQ coherences on any of the three A spins. Therefore, the three expected possibilities could be written as;

$$A_{(1)+}A_{(2)\alpha}A_{(3)\alpha} \overset{(\pi/2)_x^A}{\rightarrow} \frac{1}{32i}A_{(1)-}(A_{(2)\alpha}+A_{(2)\beta})(A_{(3)\alpha}+A_{(3)\beta}) \quad (3)$$

$$\frac{1}{32i}(A_{(1)\alpha}-A_{(1)\beta})A_{(2)-}(A_{(3)\alpha}+A_{(3)\beta}) \quad (4)$$

$$\frac{1}{32i}(A_{(1)\alpha}-A_{(1)\beta})(A_{(2)\alpha}+A_{(2)\beta})A_{(3)-} \quad (5)$$

The Eq. (3) gives a triplet with an intensity ratio 1:2:1. The separation between the two adjacent transitions of the triplet provides the coupling $^2T_{AA}$. Eqs. (4) and (5) are degenerate and each of these provides a triplet pertaining to larger separation $2(^2T_{AA})$ with an intensity ratio of −1:0:1. The detected spectrum is the cumulative addition of all the sub-spectra originating from Eqs. (3)–(5) and gives rise to a triplet of intensity −1:2:3. The origin of this triplet for A_3 region is schematically depicted in Fig. 4B. Since the spectrum is represented in the magnitude mode, a triplet with an intensity ratio of 1:2:3 is observed. It may be pointed out that a similar anomalous intensity pattern is also observed in DQ-SERF [23] and Soft-COSY [28] spectra for the experiments involving selective excitation of methyl protons. This point is completely ignored in the earlier studies. The above-mentioned polarization operator product equations could be extended to analyze the intensity pattern encountered in such experiments.

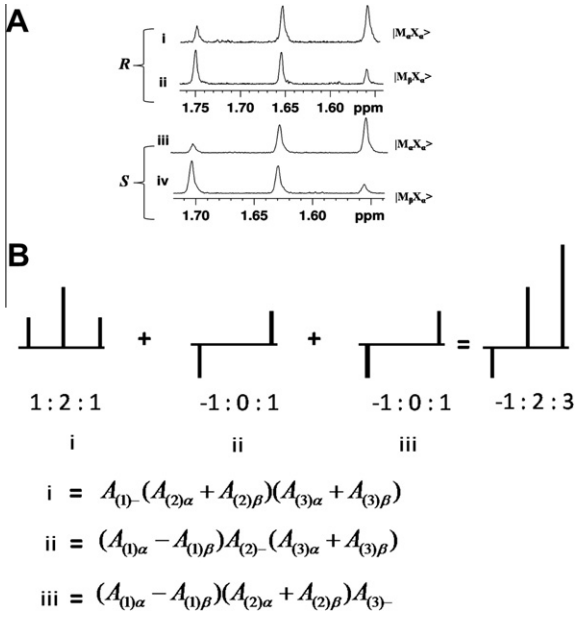

Fig. 4. (A) Cross sections taken from Fig. 3B. (i) and (ii) are for *R* enantiomer and (iii) and (iv) are for *S* enantiomers. Notice the reduction in the intensity of the triplets from high field to low field for cross sections marked (i) and (iii) *R* enantiomer or vice versa for cross sections marked (ii) and (iv) for *S* enantiomer. The passive spin states for different cross sections have been marked. (B) Pictorial representation depicting the observed −1:2:3 intensity patterns in the strongly coupled (A_3) methyl groups. (i), (ii) and (iii) are the polarization operator terms and are given below. The expected spectrum from each of the three polarization operator terms and the final detected spectrum, which is the sum of all these are depicted. The magnitude representation of the spectrum results in the triplet with the intensity pattern of 1:2:3.

4.3. Application to (R/S)-propylene carbonate

To demonstrate the robustness of the pulse sequence another molecule, (*R*/*S*)-propylene carbonate that contains IS, I_2S and I_3S groups with ^{13}C in natural abundance, which gives rise to more overcrowded ^1H NMR spectrum compared to the molecule discussed in the previous section has been investigated. The protons and ^{13}C bonded to the methyl protons of this molecule corresponds to the spin system of type A_3MNPX where A_3 spins are methyl protons, M and N are methylene protons, *P* is methine proton and *X* is the ^{13}C bonded to A_3 group. The methyl protons are coupled to *M*, *N* and *P* spins in the PBLG/$CDCl_3$ mesophase. Since the magnetically equivalent methyl protons give rise to a triplet in liquid crystalline phase, there are 24 possible transitions observed for each enantiomer at the methyl chemical shift. Consequent to coupling with directly bonded carbon, there are 48 transitions for each enantiomer. Thus the methyl region of the spectrum contains a total of 96 transitions that are severely overlapped. The analysis of such a spectrum requires the demixing of spectral overlap arising from the enantiomeric mixture. The CESS-COSY was therefore employed and the methyl selective spectrum is reported in Fig. 5. The $^2T_{HH}$ and $^1T_{CH}$ are active couplings, whereas $^3T_{HH}$, and $^4T_{HH}$ constitute the passive couplings. The spectrum can be construed as an array of 16 A_3 subspectra displaced in both the dimensions pertaining to 16 possible spin states of *M*, *N*, *P* and *X* for each enantiomer. The displacement between two identical cross sections pertaining to $|\alpha\rangle$ and $|\beta\rangle$ domains of ^{13}C provides the active coupling $^1T_{CH}$. The separations marked "*a*" and "*b*" provide this parameter respectively for *R* and *S* enantiomers.

Analysis of the region of the spectrum marked with broken rectangle in $|\alpha\rangle$ spin state of ^{13}C which is expanded in the inset of the figure provides homonuclear couplings. Separations marked "*c*" and "*f*" denotes respectively the active coupling $^2T_{HH}$ responsible for the triplet in each cross section for *R* and *S* enantiomers. The

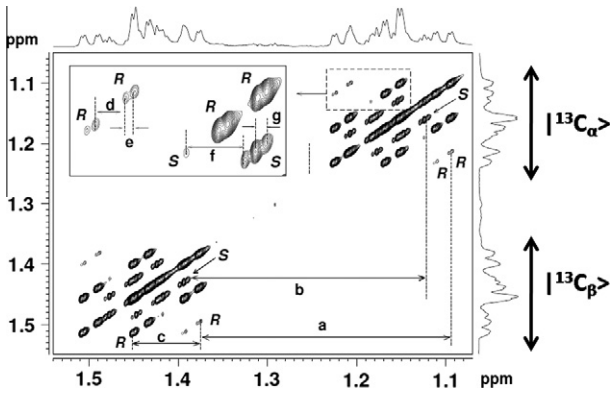

Fig. 5. The 2D CESS-COSY spectrum with selective excitation of methyl protons of (*R*/*S*)-propylene carbonate (structure given in Fig. 1) dissolved in PBLG/ $CDCl_3$ solvent, recorded at 300 K. The $|^{13}C_\alpha>$ and $|^{13}C_\beta>$ regions are marked in the F_1 dimension. Representative peaks for *R* and *S* enantiomers are marked. Broken rectangle in $|^{13}C_\alpha>$ region is expanded as an inset in the figure. The separations providing the magnitudes of the couplings and their values (in Hz) are; $a = (^1T_{CH})^R = 140.8$, $c = (^2T_{HH})^R = 27.7$, $d = (^3T_{HH})^R = 8.6$, $e = (^4T_{HH})^R = 1.9$ and $b = (^1T_{CH})^S = 134.6$, $f = (^2T_{HH})^S = 12.7$ and $g = (^3T_{HH})^S = 2.3$.

separations d and e provide the passive couplings $^3T_{HH}$ and $^4T_{HH}$ for the *R* enantiomer. Similarly, the separation "*g*" provides $^3T_{HH}$ for the *S* enantiomer. However, the coupling $^4T_{HH}$ is not derivable for the *S* enantiomer because of negligibly smaller value and is hidden within the line width.

5. Biselective excitation of diastereomeric protons

Diastereomeric protons constitute a building block of many organic chiral molecules. Therefore, we wanted to explore whether the one bond heteronuclear couplings of diastereotopic protons can be utilized for discrimination of enantiomers. In this context, the proposed experiment appears to be very promising as it permits the individual determination of one bond proton–carbon couplings for each diastereomeric proton. For the demonstration of this application we have chosen another molecule providing a complex spectrum viz., (*R*/*S*)-β-butyrolactone, which is also an A_3MNPX system. Due to large difference in the resonance frequencies of diastereomeric protons the simultaneous excitation of these two protons requires biselective pulse.

The protons H6 and H7 biselectively excited 2D CESS-COSY spectrum of (*R*/*S*)-β-butyrolactone aligned in PBLG/$CDCl_3$ mesophase is reported in Fig. 6A. The spectrum at H6 chemical shift consists of a doublet with a larger separation arising due to active coupling with its directly bonded ^{13}C (carbon numbered 3). This is further split into another doublet by its geminal coupling with H7 proton. The each component of this doublet of a doublet is further split into another doublet due to passive coupling with proton H5 which is displaced along the F_1 dimension. Finally, each component of this multiplet is split further into a quartet due to passive coupling with proton H4 which is also displaced along the F_1 dimension. The complete demixing of the transitions is very clear from the quality of the spectrum. The spectrum provides two active couplings $^1T_{C3H6}$ and $^2T_{H6H7}$ and two passive couplings $^2T_{H6H5}$ and $^2T_{H6H4}$. Likewise, the spectrum at H7 chemical shift could be understood and provides two active couplings $^1T_{C3H7}$ and $^2T_{H6H7}$ and two passive couplings $^2T_{H7H5}$ and $^2T_{H7H4}$. All derivable coupling parameters are represented in Fig. 6B and C.

6. Heteronuclear decoupling in the indirect dimension

Employment of heteronuclear decoupling in the indirect dimension of the above experiment has additional advantages such as; (a) it employs difference in ^1H–^1H couplings for the enantiomers in the indirect dimension and utilizes the differential values of both ^1H–^1H and ^1H–^{13}C couplings as discriminating parameters in the direct dimensions. This gives rise to the demixing of severely overlapping signals observed in the CESS-COSY 2D spectrum, (b) it demands less number of t_1 data points in the indirect dimension consequent to reduced spectral width resulting in saving of experimental time and (c) all the possible couplings obtainable from the CESS-COSY experiment can also be extracted from the hetero-decoupled CESS–COSY experiment. This is experimentally demonstrated by employing the pulse sequence depicted in Fig. 2B. The hetero-decoupled CESS-COSY spectrum of the methyl selective (*R*/*S*)-propylene carbonate is reported in Fig. 7A. Analysis of the spectrum is identical to methyl selective CESS-COSY of this molecule in the direct dimension. The spectrum differs only in the indirect dimension consequent to the absence of ^{13}C–^1H coupling. The separations marked "*a*" and "*b*" denotes the heteronuclear one bond ^{13}C–^1H total couplings $(^1T_{CH})^{R/S}$. Furthermore, since the selective pulse has been realized only on methyl protons, the two non-equivalent methylene protons and methine proton constitute the passive spins in the indirect dimension. Therefore, the spectrum pertains to the A_3 part of the A_3MNX spin system containing 24 transitions in the indirect dimension which can be construed as eight A_3 sub-spectra corresponding to eight spin states of *M*, *N*, and *X*. The spectrum at $|^{13}C_\beta>$ spin state of the methyl carbon along the F_2 dimension is expanded in Fig. 7B. Each cross section taken parallel to the F_2 dimension, is a triplet which provides the active coupling among the methyl protons. The separations marked "*c*" and "*e*" denote $^2T_{H4H4}$ for *R* and *S* enantiomers, respectively. The separation "*d*" and "*f*" represent the passive coupling between the methyl and methine protons $(^3T_{HH})^{R/S}$. The other long-range couplings $^4T_{H4H6}$ and $^4T_{H4H7}$ are not derivable because of their negligibly smaller values.

The advantage of this experiment becomes obvious when compared with Soft-COSY experiment demonstrated for chiral analysis [23]. The methyl selective soft-COSY spectrum of this molecule recorded using the well known pulse sequence [22–25] is given in Fig. 7C. It consists of two semi-selective pulses applied on methyl multiplets separated by an evolution delay. The appearance of the spectrum is similar to the indirect dimension of the hetero-decoupled CESS-COSY experiment. From the spectrum, it is clear that diagonal peaks inside broken rectangles are severely overlapped and the visualization of the enantiomers is not possible. On the other hand in hetero-decoupled CESS-COSY, these peaks are well resolved (Fig. 6B) enabling chiral differentiation. This is mainly due to difference of the ^{13}C–^1H couplings between the enantiomers [i.e. $(^1T_{CH})^R - (^1T_{CH})^S = 6.2$ Hz] in the direct dimension. As far as the sensitivities of the CESS-COSY and Soft-COSY experiments are concerned, it may be pointed out that the sensitivity of Soft-COSY experiment is several orders of magnitude higher.

It can also be argued that HSQC experiment without decoupling in the direct dimension could be used for the extraction of couplings. The present experiment finds significant advantage over the HSQC experiment because of the appearance of the spectrum in different cross sections in the direct dimension. As an example, in the F2HSQC spectrum of (*R*/*S*)-propylene carbonate, there are 48 transitions in one cross section at the chemical shift position of methyl protons for each enantiomer making precise measurement of coupling difficult, whereas in the methyl selective CESS-COSY spectrum, these 48 transitions appears in 16 different cross sections. This is a significant advantage in the precise measurement of couplings of smaller magnitudes.

Another common problem associated with conventional HSQC experiments carried out on partially oriented samples is the encyclopedic spread of heteronuclear one-bond couplings [29]. Therefore, there is signal loss due to mismatched delay in the back

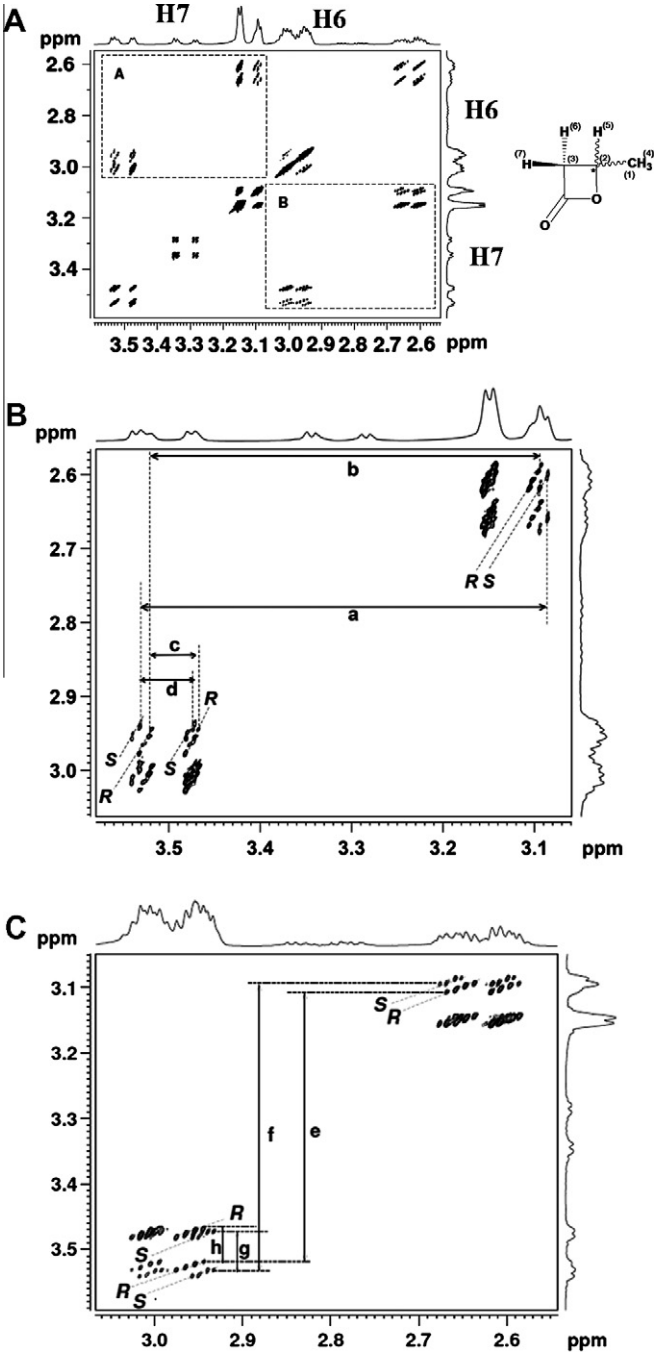

Fig. 6. (A) The 2D CESS-COSY spectrum of (*R*/*S*)-β-butyrolactone aligned in PBLG/ $CDCl_3$ mesophase, utilizing biselective excitation of diastereomeric protons H6 and H7, recorded at 300 K. The chemical structure and the number of the interacting protons and the participating ^{13}C spin are given adjacent to the 2D matrix. (B) Expanded region A of the spectrum marked with broken rectangle in Fig. 6A. Few representative peaks for *R* and *S* enantiomers have been identified. The separations providing the magnitudes of the couplings and their values (in Hz) are; $a = (^1T_{C3H7})^R = 214.2$, $b = (^1T_{CH})^S = 223.3$, $c = (^2T_{H6H7})^R = 31.2$ and $d = (^2T_{H6H7})^S = 20.2$. (C) Expanded region B of the spectrum marked with broken rectangle in Fig. 6A. The separations providing the magnitudes of the couplings and their values (in Hz) are; $e = (^1T_{C3H6})^R = 207.4$, $f = (^1T_{CH6})^S = 219.14$, $g = (^2T_{H6H7})^S = 20.2$ and $h = (^2T_{H6H7})^R = 31.2$.

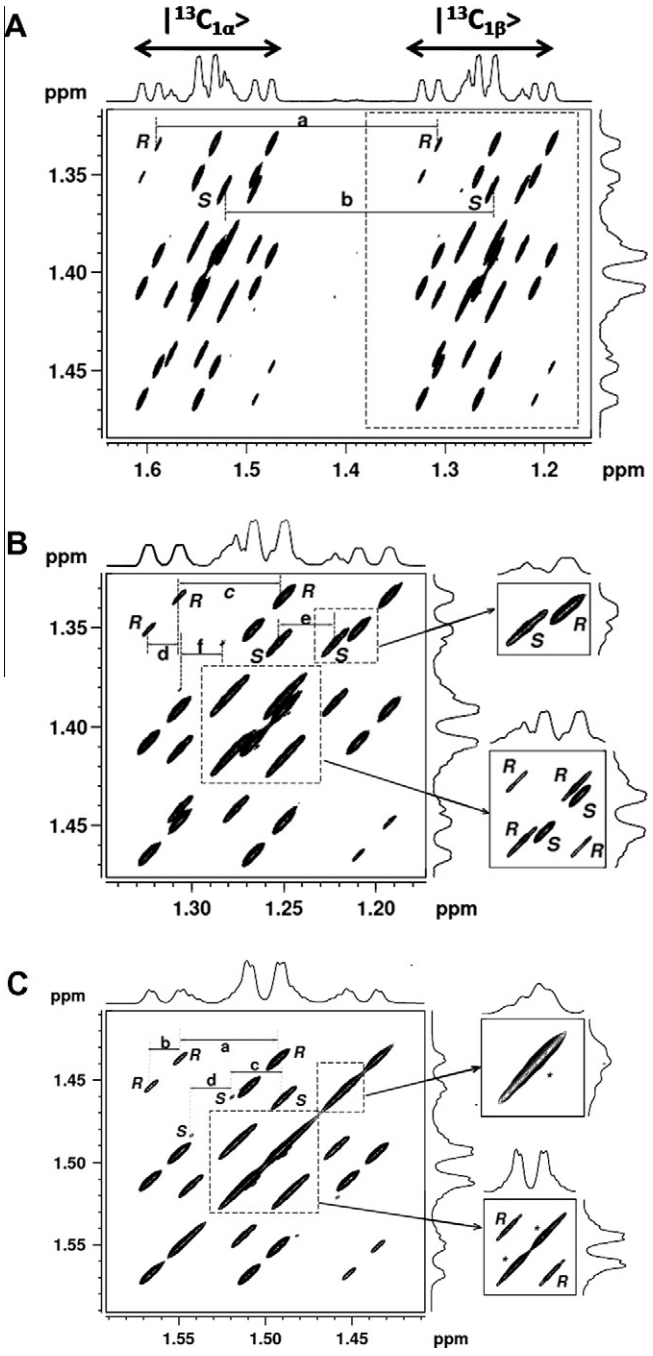

Fig. 7. (A) The ^{13}C decoupled 2D CESS-COSY spectrum with selective excitation of methyl protons of (*R*/*S*)-propylene carbonate oriented in PBLG/ $CDCl_3$ solvent and recorded at 300 K. The 2D data matrix size is 1004 × 256. Spectral widths are respectively 100 Hz and 250 Hz in both the F_1 and F_2 dimensions. The EBURP-2 shaped pulse of duration 3.15 ms was used to excite the multiplet of methyl protons. The relaxation delay was 2.5 s and number of accumulation was 8. The data was zero-filled to 2048 and 4096 and processed with a sine bell window function. The $|^{13}C_\alpha>$ and $|^{13}C_\beta>$ regions are marked in the F_2 dimension. Representative peaks for *R* and *S* enantiomers are marked. The separation providing the couplings (in Hz) are $a = (^1T_{CH})^R = 140.8$ and $b = (^1T_{CH})^S = 134.6$ (B) The expansion of $|^{13}C_\beta>$ region of Fig. 6A. The separations providing the magnitudes of the couplings and their values (in Hz) are; $c = (^2T_{HH})^R = 27.7$, $d = (^3T_{HH})^R = 8.6$ and $e = (^2T_{HH})^S = 12.7$ and $f = (^3T_{HH})^R = 10.7$ (C) The methyl selective Soft-COSY spectrum of (*R*/*S*)-propylene carbonate. The EBURP-2 and U-BURP shaped pulses of 3.15 ms were used for the preparation and mixing. The 2D data matrix size is 900 × 256. Spectral widths are 100 Hz in both the F_1 and F_2 dimensions. The number of accumulations for each t_1 increment is 4. The relaxation delay is 2.5 s. The data was zero-filled to 2048 and 4096 and processed with a sine bell window function. The peaks marked * have the overlapping *R*/*S* signals. The markings providing the couplings (in Hz) are $a = (^2T_{HH})^R = 27.7$, $b = (^3T_{HH})^R = 8.6$ and $c = (^2T_{HH})^S = 12.7$ and $d = (^3T_{HH})^R = 10.7$.

transfer of INEPT. Here, again, the present experiment has a significant advantage over other HSQC-based schemes since it needs only a single INEPT step to prepare ^{13}C edited proton magnetization and there is no need to optimize the delay for the back transfer. Furthermore, it is devoid of long-range cross peaks often encountered in the HSQC experiment between carbon and

remotely coupled protons in the oriented sample [30]. It is primarily because of the selective retention of coupling in CESS-COSY experiment by the application of semi-selective pulses.

It may be pointed out that the phased two dimensional spectra provide high resolution and permits the extraction of couplings of smaller magnitude. The magnitude mode representation of the present methodology is sufficient to extract even the couplings of very small magnitudes in small chiral molecule embedded in chiral liquid crystal analogous to that of phased spectrum. In addition, the long phase cycling required in obtaining phased spectrum in ^{13}C natural abundance demands enormous amount of instrument time. Therefore no attempt is made to obtain the phased spectrum.

Also major limitation of this kind of experiment is it works only when the one dimensional spectra contains complex resolved lines for different groups of protons. Furthermore, there is a non-uniform transfer of magnetization in the INEPT block because of differential value of $^1T_{CH}$. Therefore, the quantification of enantiomeric excess (ee) by this experiment may not be precise. It could be pointed out that employment of uniform evolution of magnetization like in quantitative HSQC [31] experiment enables the precise measurement of ee. The aim of the present study is to develop method for demixing of the overlap and not the measure of enantiomeric content. However, there are a few two dimensional experiments such as SERF, Soft-COSY which provide ee with 2–5% error [13,23]. On the other hand when NADNMR is employed, the well resolved quadrupole doublets for each chemically independent ^2H, absence of ^2H–^2H interactions, enable precise measure of 'ee', even though sensitivity of ^2H detection is several orders of magnitude smaller than ^1H detection. Therefore, if one is interested in the precise measurement of enantiomeric excess, NADNMR is an excellent alternate [9].

7. Conclusions

An experiment is proposed which involves the single carbon edited selectively excited proton–proton correlation of weakly dipolar coupled spins. The technique demixes the severely overlapped peaks in the very intricate ^{13}C coupled proton NMR spectra of enantiomers. It also permits the determination of both residual homonuclear and one bond carbon-proton heteronuclear couplings in I_2S and I_3S groups. The chiral discrimination, utilizing exclusively diastereomeric protons which are most often encountered in all chiral organic molecules, is also demonstrated. The employment of additional proton–carbon decoupling in indirect dimension results in better and unambiguous chiral visualization unlike experiments which utilize only homonuclear proton couplings. This experiment has been demonstrated to be superior over methyl selective Soft-COSY experiment. The experiment is simple, robust and easy to implement.

Acknowledgments

NN would like to thank UGC, India for a senior research fellowship. NS gratefully acknowledges the financial support by Board of Research in Nuclear Sciences, Mumbai, for the Grant No. 2009/37/38/BRNS/2269.

References

[1] T. Ohtaki, K. Akasaka, C. Kabuto, H. Ohrui, Chiral discrimination of secondary alcohols by both ^1H-NMR and HPLC after labeling with a chiral derivatization reagent, 2-(2,3-anthracenedicarboximide) cyclohexane carboxylic acid, Chirality 17 (2005) S171–176.
[2] D. Parker, NMR determination of enantiomeric purity, Chem. Rev. 91 (1991) 1441–1457.
[3] C. Aroulanda, M. Sarfati, J. Courtieu, P. Lesot, Investigation of the enantioselectivity of three polypeptides liquid crystal solvents using NMR spectroscopy, Enantiomer 6 (2001) 281–287.
[4] M. Sarfati, P. Lesot, D. Merlet, J. Courtieu, Theoretical and experimental aspects of enantiomeric differentiation using natural abundance multinuclear NMR spectroscopy in chiral polypeptide liquid crystals, Chem. Comm. (2000) 2069–2081.
[5] I. Canet, J. Courtieu, A. Loewenstein, A. Meddour, J.M. Péchiné, Enantiomeric analysis in a polypeptide lyotropic liquid crystal by deuterium NMR, J. Am. Chem. Soc. 117 (1995) 6520–6521.
[6] P. Lesot, M. Sarfati, D. Merlet, B. Ancian, J. Emsley, B.A. Timimi, 2D-NMR strategy dedicated to the analysis of weakly ordered, fully deuterated enantiomers in chiral liquid crystals, J. Am. Chem. Soc. 125 (2003) 7689–7695.
[7] D. Merlet, M. Sarfati, B. Ancian, J. Courtieu, P. Lesot, Description of natural abundance deuterium 2D-NMR experiments in weakly ordered liquid-crystalline solvents using a tailored Cartesian spin-operator formalism, Phys. Chem. Chem. Phys. 2 (2000) 2283–2290.
[8] P. Lesot, O. Lafon, Enantiomeric analysis using natural abundance deuterium 3D NMR spectroscopy in polypeptide chiral oriented media, Chem. Phys. Lett. 458 (2008) 219–222.
[9] P. Lesot, J. Courtieu, Natural abundance deuterium NMR spectroscopy: developments and analytical applications in liquids, liquid crystals and solid phases, Prog. Nucl. Magn. Reson. Spect. 55 (2009) 128–159.
[10] A. Meddour, P. Berdague, A. Hedli, J. Courtieu, P. Lesot, Proton–decoupled carbon-13 NMR spectroscopy in a lyotropic chiral nematic solvent as an analytical tool for the measurement of the enantiomeric excess, J. Am. Chem. Soc. 119 (1997) 4502–4508.
[11] J. Farjon, L. Ziani, L. Beguin, D. Merlet, J. Courtieu, Selective NMR excitations in chiral analysis, Ann. Rep. NMR Spect. 61 (2007) 283–293.
[12] N. Giraud, M. Joos, J. Courtieu, D. Merlet, Application of a ^1H δ-resolved 2D NMR experiment, to the visualization of enantiomers in chiral environment using sample spatial encoding and selective echoes, Magn. Reson. Chem. 47 (2009) 300–306.
[13] J. Farjon, D. Merlet, P. Lesot, J. Courtieu, Enantiomeric excess measurements in weakly oriented chiral liquid crystal solvents through $2D^1H$ selective refocusing experiments, J. Magn. Reson. 158 (2002) 169–172.
[14] N. Nilamoni, N. Suryaprakash, Selective detection of single-enantiomer spectrum of chiral molecules aligned in the polypeptide liquid crystalline solvent: transition selective one-dimensional ^1H–^1H COSY, J. Magn. Reson. 202 (2010) 34–37.
[15] C. Griesinger, O.W. Sørensen, R.R. Ernst, Two-dimensional correlation of connected NMR transitions, J. Am. Chem. Soc. 107 (1985) 6394–6396.
[16] C. Griesinger, O. W Sørensen, R.R. Ernst, Correlation of connected transitions by two-dimensional NMR spectroscopy, J. Chem. Phys. 85 (1986) 6837–6852.
[17] P. Lesot, D. Merlet, J. Courtieu, J.W. Emsley, Discrimination and analysis of the NMR Spectra of enantiomers dissolved in chiral liquid crystal solvents trough 2D correlation experiments, Liquid Cryst. 21 (3) (1996) 427–435.
[18] L. Ziani, J. Courtieu, D. Merlet, Visualization of enantiomers via insertion of a BIRD module in X–H correlation experiments in chiral liquid crystal solvent, J. Magn. Reson. 183 (2006) 60–67.
[19] B. Bikash, R.P. Uday, N. Suryaprakash, Binuclear spin state selective detection of ^1H single quantum transitions using triple quantum coherence: a novel method for enantiomeric discrimination, J. Magn. Reson. 192 (2008) 92–100.
[20] V.M. Marathias, I. Goljer, A.C. Bach II, Simultaneous determination of ^1H–^1H and ^1H–^{13}C residual dipolar couplings in a chiral liquid crystal solvent using a natural abundance HSQC experiment, Magn. Reson. Chem. 43 (2005) 512–519.
[21] V.M. Marathias, G.J. Tawa, I. Goljer, A.C. Bach II, Stereochemical identification of (*R*)- and (*S*)-Ibuprofen using residual dipolar couplings, NMR, and modeling, Chirality. 19 (2007) 741–750.
[22] J. Cavanagh, J.P. Waltho, J. Keeler, Semiselective two-dimensional NMR experiments, J. Magn. Reson. 74 (1987) 386–393.
[23] R.P. Uday, B. Bikash, N. Suryaprakash, Separation and complete analyses of the overlapped and unresolved ^1H NMR spectra of enantiomers by spin selected correlation experiments, J. Phys. Chem. A. 112 (2008) 5658–5669.
[24] L. Emsley, G. Bodenhausen, Self-refocusing effect of 2700°Gaussian pulses. Applications to selective two-dimensional exchange spectroscopy, J. Magn. Reson. 82 (1989) 211–221.
[25] R. Brüschweiler, J.C. Madsen, C. Griesinger, O.W. Sørensen, R.R. Ernst, Two-dimensional NMR spectroscopy with soft pulses, J. Magn. Reson. 73 (1987) 380–385.
[26] G.A. Morris, R. Freeman, Enhancement of nuclear magnetic resonance signals by polarization transfer, J. Am. Chem. Soc. 101 (1979) 760–762.
[27] J. Keeler, Understanding NMR Spectroscopy, John Wiley and Sons, England, 2005.
[28] B. Bikash, R.P. Uday, N. Suryaprakash, Enantiomeric discrimination by double quantum excited selective refocusing (DQ-SERF) experiment, J. Phys. Chem. B. 111 (2007) 12403–12410.
[29] T. Pavleta, S. Svetlana, L. Burkhard, P.E.HSQC: a simple experiment for simultaneous and sign-sensitive measurement of ($^1JCH + D_{CH}$) and ($^2J_{HH} + D_{HH}$) couplings, J. Magn. Reson. 186 (2007) 193–200.
[30] E. Andreas, F.J. Christoph, F. Julien, K. Horst, L. Burkhard, The CLIP/CLAP-HSQC: pure absorptive spectra for the measurement of one-bond couplings, J. Magn. Reson. 192 (2008) 314–322.
[31] S. Heikkinen, M.M. Toikka, P.T. Karhunen, I. Kilpeläinen, Quantitative 2D HSQC (Q-HSQC) via suppression of J-dependence of polarization transfer in NMR spectroscopy: application to wood lignin, J. Am. Chem. Soc. 125 (2003) 4362–4367.